J Neuropathol Exp Neurol

Vol. 70, No. 4
April 2011
pp. 253–263

ORIGINAL ARTICLE

# Mitochondrial Dysfunction and Oxidative and Endoplasmic Reticulum Stress in Argyrophilic Grain Disease

Ekaterina V. Ilieva, PhD, Anton Kichev, PhD, Alba Naudí, PhD, Isidre Ferrer, MD, PhD, Reinald Pamplona, MD, PhD, and Manuel Portero-Otín, MD, PhD

**Abstract**

Argyrophilic grain disease (AGD) is characterized by the accumulation of hyperphosphorylated 4R tau in dendritic varicosities (i.e. ''grains'') in neurons and pretangles in certain areas of the cerebral cortex and other brain regions. We investigated oxidative and endoplasmic reticulum (ER) stress and dysregulation of mitochondrial biogenesis as potential mechanisms involved in the AGD pathogenesis. Samples from AGD patients (n = 8) and nonpathologic, age-matched controls (n = 5) were compared using biochemical and immunohistochemical techniques with a panel of antibodies to markers of ER stress responses, stress chaperones, oxidative stress and associated cellular responses, respiratory chain complexes, mitochondrial regulators, and modulators of mitochondrial biogenesis. Because AGD is often associated with other tauopathies, mainly Alzheimer disease (AD), results were also compared with those of a group of similar Braak AD stage cases without grains (n = 5). In both AD and AGD cases, we found activation of key molecules that are involved in the unfolded protein response and lead to elevated ER chaperone levels, increased oxidative stress damage, mainly related to lipoxidation and targeting glycolytic enzymes. Altered expression of components of the respiratory chain markers modulating mitochondrial biogenesis were selectively affected in AGD. The findings suggest that, despite the common pathogenic trends in AD and AGD, there is molecular specificity for AGD.

From the Department of Experimental Medicine (EVI, AK, AN, RP, MP-O), University of Lleida-Irblleida, Lleida; and Institute of Neuropathology (IF), Service of Pathologic Anatomy, IDIBELL-University Hospital of Bellvitge, University of Barcelona, CIBERNED - carrer Feixa Llarga sn, Hospitalet de Llobregat, Barcelona, Spain.

Send correspondence and reprint requests to: Manuel Portero-Otín, MD, PhD, Department of Experimental Medicine, University of Lleida-Irblleida, C/Montserrat Roig, 2, Lleida 25008, Spain; E-mail: manuel.portero@mex.udl.cat

Supported by research and development grants from the Spanish Ministry of Education and Science (BFU2009-11879/BFI; AGL2006-12433), the Generalitat of Catalunya (2009SGR-735), the Spanish Ministry of Health (FIS 05-2241, 05-1570, 08-1843, RD06/0013/0012), and ''La Caixa'' Foundation to Reinald Pamplona and Manuel Portero-Otín; the Spanish Ministry of Health (FIS 08-582) and the European Commission under the VI Framework Programme (BrainNet Europe II, LSHM-CT- 2004-503039) to Isidre Ferrer; and the BESAD-P project (Carlos III Institute) to Isidre Ferrer, Reinald Pamplona and Manuel Portero-Otín. Ekaterina V. Ilieva is a predoctoral fellow from the Generalitat de Catalunya. Supported also by the COST B-35 Action.

Supplemental digital content is available for this article. Direct URL citations appear in the printed text and are provided in the HTML and PDF versions of this article on the journal's Web site (www.jneuropath.com).

**Key Words**: Argyrophilic grain disease, Endoplasmic reticulum stress, Mitochondrial dysfunction, Neurodegeneration, Oxidative stress, Proteomics, Unfolded protein response.

## INTRODUCTION

Argyrophilic grain disease (AGD) is a neurodegenerative condition morphologically characterized by the presence of 4R hyperphosphorylated tau protein in neuritic swellings known as argyrophilic grains, neurons with pretangles, coiled bodies in oligodendrocytes, and hyperphosphorylated tau-immunoreactive astrocytes located predominantly in brain limbic regions (1, 2). Argyrophilic grain disease is positively correlated with advancing age, and it is often associated with other neurodegenerative diseases, including Alzheimer disease (AD) and other tauopathies and synucleinopathies (1, 3). Argyrophilic grain disease stage 1 affects the anterior entorhinal cortex, part of the cortical and basolateral nuclei of the amygdala, and the hypothalamic lateral tuberal nucleus. Stage 2 involves more numerous lesions with progression to the whole entorhinal cortex, anterior CA1, transentorhinal cortex, cortical and basolateral nuclei of the amygdala, presubiculum, hypothalamic lateral tuberal nucleus, and dentate gyrus. Stage 3 further involves CA1, perirhinal cortex, presubiculum, amygdala, dentate gyrus, hypothalamic lateral tuberal nucleus, CA2 and CA3, subiculum, other nuclei of the hypothalamus (e.g. mamillary bodies), anterior temporal cortex, insular cortex, anterior cingulate gyrus, orbitofrontal cortex, nucleus accumbens, and septal nuclei. Stage 4 is characterized by moderate to severe additional involvement of the neocortex and brainstem (1–3).

Aging nervous system cells undergo oxidative stress (4), accumulation of damaged proteins (5, 6), mitochondrial dysfunction (7), and decreased proteasomal activity (8, 9). Oxidative protein damage arises from direct exposure to reactive oxygen species that generate oxidative products such as glutamic (GSA) and aminoadipic (AASA) semialdehydes (10–12). Protein modifications may also arise from reactions with low-molecular weight and highly reactive carbonyl compounds derived from carbohydrates or polyunsaturated fatty acid oxidation in processes termed ''glyco-'' and ''lipoxidation,'' respectively. These reactions can lead to the formation of specific adducts, such as *N*ϵ-carboxymethyl-lysine (CML), *N*ϵ-carboxyethyl-lysine (CEL), and *N*ϵ-malondialdehyde-lysine (MDAL) (13, 14). Endoplasmic reticulum (ER) stress is

induced by the disruption of ER-associated degradation, a pathway the helps to clear misfolded proteins from the ER (15, 16). The expression of mutant ubiquitin resulting from messenger RNA misreading and ubiquitin deposits that may indicate impaired proteasomal function has been observed in AGD (1).

Oxidative and ER stress are also considered to play roles in the pathogenesis of AD, amyotrophic lateral sclerosis, Pick disease, and many other neurodegenerative diseases (17–22), but little is known about their role in AGD. To obtain an overall view of modifications in the hippocampus in AGD, we examined expression levels of different proteins related to ER stress, chaperone function, oxidative damage markers, mitochondrial subunits of respiratory chain complexes, cellular defense responses, and mitochondrial biogenesis. Because AGD is often associated with AD, we also compared these AGD samples with AD-only cases with similar Braak stages to those in the AGD group.

## MATERIALS AND METHODS

### Case Material

Samples of the hippocampus were obtained from the Institute of Neuropathology Brain Bank (Hospitalet de Llobregat, Barcelona, Spain) following the guidelines of the local ethics committee. The agonal state was short with no evidence of acidosis or prolonged hypoxia; the pH of each brain was between 6.8 and 7. Cases of AGD (n = 8), AD-only (n = 5), and controls (n = 5) with postmortem delays between 2 and 17 hours were selected for study (Table 1). The restricted postmortem delay was within the range enabling the study of oxidative damage in the postmortem brain (23). There were 5 stage 2 AGD cases and 3 stage 3 AGD cases. All of these also had AD-related pathology Braak stage I or II (entorhinal or transentorhinal stages of neurofibrillary tangle pathology, and 0 or A of β-amyloid plaque pathology).

The AD-only cases had similar stages of neurofibrillary and β-amyloid plaque pathology (mostly Braak stages I–III/0–B). This strict selection of cases reduced the possibility of bias related to the presence of AD-related pathology in AGD. Argyrophilic grain disease cases with marked AD pathology and those with other tauopathies such as progressive supranuclear palsy or corticobasal degeneration were excluded. This design permitted a reasonable approach to the study of AGD-related changes.

Control patients had negative neurologic histories. This was further determined after the postmortem neuropathologic study by individualized interviews with the relatives. Three cases with AGD stage 2 (Cases 2, 6, and 7) were also preserved cognitively. In the other AGD cases, there were histories of altered behavior and mild or moderate cognitive impairment (e.g. eccentricities, obsessions, forgetfulness, apathy, and depression) considered to be ''related to aging.'' Dementia was not present in any case.

**TABLE 1.** Summary of Clinical and Pathologic Data

| Case No. | Age, yr | Sex | AGD Stage | Other Findings | Postmortem Delay, h |
|---|---|---|---|---|---|
| 1 | 82 | M | AGD 2 | AD I, AA | 13 |
| 2 | 74 | M | AGD 3 | AD I-0, Crib | 4 |
| 3 | 88 | F | AGD 3 | AD I-0, Crib | 9 |
| 4 | 79 | F | AGD 2 | AD II-0, Crib | 6 |
| 5 | 95 | M | AGD 2 | AD I-0, Crib | 10 |
| 6 | 66 | M | AGD 2 | AD I-A | 5 |
| 7 | 65 | F | AGD 2 | AD I-0 | 2 |
| 8 | 74 | F | AGD 3 | AD II-0 | 9 |
| 9 | 75 | F | 0 | No lesions | 3 |
| 10 | 67 | M | 0 | No lesions | 5 |
| 11 | 30 | M | 0 | No lesions | 4 |
| 12 | 63 | M | 0 | No lesions | 17 |
| 13 | 56 | F | 0 | No lesions | 9 |
| 14 | 59 | M | 0 | AD II-B | 7 |
| 15 | 74 | F | 0 | AD III | 5 |
| 16 | 72 | M | 0 | AD II-B | 10 |
| 17 | 79 | M | 0 | AD III | 4 |
| 18 | 75 | M | 0 | AD IV-A | 2 |

0, A, B, stages of amyloid plaque pathology; AA, amyloid angiopathy; AD, Alzheimer disease; AGD, argyrophilic grain disease (stage 2 and 3); Crib, status cribosus; I–II, entorhinal and transentorhinal stages of neurofibrillary pathology.

### Protein Analyses by Immunoblot

Brain samples (200 mg) from the hippocampus of AGD and control cases were prepared as previously described (17). Immunodetection was performed using the primary and secondary antibodies listed in Table 2. Protein bands were visualized with the chemiluminescence ECL method (Millipore Corporation, Billerica, MA). The monoclonal antibody to β-actin (Sigma, St Louis, MO), diluted 1:5000, was used to control protein loading. The density of each immunoreactive band was determined by densitometry analysis using a GS-800 Calibrated Densitometer (Bio-Rad, Barcelona, Spain).

### Protein Identification

Two-dimensional electrophoresis was performed as previously described (17). Immunoblot analysis was performed using a primary anti-CML polyclonal antibody. For gel staining, a MS-modified silver staining method (Amersham Biosciences, Barcelona, Spain) was used according to the manufacturer's instructions. For membrane staining, a silver staining method based on the Gallyas intensifier was used as previously described (17).

The gels and PVDF membranes were scanned using a GS800 Calibrated Densitometer (Bio-Rad). PDQuest 2-dimensional analysis software (Bio-Rad) was used for matching and analysis of silver-stained gels and membranes. The average mode of background subtraction was chosen to compare protein and CML immunoreactivity content between hippocampus samples from AGD and control patients (17).

Enzymatic digestion was performed with trypsin (Promega, Madison, WI) following conventional procedures, as previously described (24). Mass spectrometry analysis was performed using a Voyager DE-PRO MALDI-reTOF mass spectrometer (Applied Biosystems, Foster City, CA). The Protein Prospector software version 4.0.1 (University of

**TABLE 2.** Antibodies and Conditions Used for Western Blotting

| Antigen | Supplier | Dilution |
|---|---|---|
| Phosphorylated (S52) eIF2α | Cell Signaling, Beverly, MA | 1:1000 |
| eIF2α | Cell Signaling | 1:1000 |
| IRE 1 | ProSci, San Diego, CA | 1:1000 |
| XBP1 | ProSci | 1:1000 |
| ATF6α | ProSci | 1:1000 |
| Grp78/BiP | Stressgen, Brussels, Belgium | 1:1000 |
| Grp94 | Santa Cruz Biotechnology, Santa Cruz, CA | 1:500 |
| PDI | Abcam, Cambridge, UK | 1:250 |
| Mitochondrial complex I (NDUFS3 subunit) | Invitrogen, Carlsbad, CA | 1:2000 |
| Mitochondrial complex II (SDHA subunit) | Invitrogen | 1:1000 |
| Mitochondrial complex III (UQCRC2 subunit) | Invitrogen | 1:2000 |
| Mitochondrial complex IV (MTCO1 subunit) | Invitrogen | 1:1000 |
| Nrf1 | Santa Cruz | 1:200 |
| NRF2 | Santa Cruz | 1:750 |
| PGC1α | Santa Cruz | 1:200 |
| AIF (apoptosis-inducing factor) | Sigma, St Louis, MO | 1:5000 |
| Mfn1 | Santa Cruz | 1:200 |
| TFAM | Santa Cruz | 1:200 |
| Sirt 1 | Santa Cruz | 1:200 |
| UCP 4 | Santa Cruz | 1:200 |
| β-Actin | Sigma | 1:5000 |
| Porin | Invitrogen | 1:5000 |
| CEL | TransGenic, Inc, Kumamoto, Japan | 1:1000 |
| CML | Academy Bio-Medical Co, Houston, TX | 1:1000 |
| MDA-Lys | Academy Bio-Medical Co | 1:1000 |
| KDEL | Abcam | 1:250 |
| DNP | Sigma | 1:2500 |
| Anti-mouse | Amersham | 1:30000 |
| Anti-rabbit | Pierce | 1:100000 |
| Anti-goat | Vector Laboratories, Burlingame, CA | 1:15000 |

ATF6, activating transcription factor 6; CML, *N*ε-carboxymethyl-lysine; CEL, *N*ε-carboxyethyl-lysine; eIF-2α, eukaryotic translation initiation factor 2 α subunit; Grp78/BiP, glucose-regulated protein 78/ immunoglobulin heavy chain binding protein; Grp94, glucose-regulated protein 94; IRE1, inositol requiring 1; MDAL, *N*ε-malondialdehyde-lysine; Mfn1, mitochondrial fusion protein-1; MTCO1, mitochondrially encoded cytochrome *c* oxidase I; Nrf1, nuclear respiratory factor 1; NRF2, nuclear factor (erythroid-derived 2)-like 2; NDUFS3, NADH dehydrogenase (ubiquinone) Fe-S protein 3; PDI, protein disulfide isomerase; p-eIF-2α, phosphorylated eukaryotic translation initiation factor 2 α subunit; PERK, double-stranded RNA-activated protein kinase–like ER kinase; PGC1α, peroxisome proliferator–activated receptor-coactivator-1; RIP140, receptor interacting protein 140; SDHA, succinate dehydrogenase complex, subunit A; SIRT1, sirtuin 1; TFAM, mitochondrial transcriptional factor A; UCP4, uncoupling protein 4; UQCRC2, ubiquinol-cytochrome *c* reductase core protein II; XBP1, x-box binding protein 1.

California San Francisco, Mass Spectrometry Facility, CA) was used to identify proteins from the peptide mass fingerprinting obtained from MALDI-reTOF MS. Swiss-Prot (European Bioinformatics Institute, Heidelberg, Germany) and GenBank (National Center for Biotechnology Information, Bethesda, MD) databases were used for the search.

## Immunohistochemistry and Double-Labeling Immunofluorescence and Confocal Microscopy

For immunohistochemistry, dewaxed 5-μm-thick sections were processed following the EnVision + system peroxidase procedure (Dako, Barcelona, Spain). After incubation with methanol and normal serum, the sections were incubated with the appropriate primary antibody at 4°C overnight. Primary antibodies included rabbit polyclonal mitochondrial porin (Abcam, Cambridge, UK; 1:2000), mouse monoclonal cytochrome *C* oxidase subunit IV (COX; Molecular Probes, Leiden, the Netherlands; 1:1000), phospho-tau (AT8; Inverness Medical, Hospitalet de Llobregat, Spain; 1:50), polyclonal phospho-tau Thr181 (tauThr181; Calbiochem, San Diego, CA; 1:500), goat polyclonal anti–superoxide dismutase 1 (SOD1) (Novocastra, Servicios Hospitalarios, Barcelona, Spain; 1:100) and rabbit polyclonal anti-SOD2 (Stressgen, Barcelona, Spain; 1:500). After washing with PBS, the sections were incubated in a cocktail of secondary antibodies diluted in vehicle solution for 3 hours at room temperature. To rule out nonspecific staining, control sections were incubated with the secondary antibodies alone. Nuclei were stained with TO-PRO.

## Measurement of Specific Protein Oxidation–Derived Markers and Fatty Acid Composition

For this study, GSA, AASA, CML, CEL, and MDAL were determined as trifluoroacetic acid methyl ester derivatives in acid-hydrolyzed delipidated and reduced protein samples by gas-chromatography mass spectrometry (17), using a HP6890 Series II gas chromatograph (Agilent, Barcelona, Spain) with a MSD5973A Series and a 7683 Series automatic injector, a HP-5MS column (30 m × 0.25 mm × 0.25 μm) and the described temperature program (17). Quantification was performed by internal and external standardization using standard curves constructed from mixtures of deuterated and nondeuterated standards. Product amounts were expressed as the micromolar ratio of GSA, AASA, CML, CEL, or MDAL per mol of lysine.

Fatty acyl groups of hippocampal lipids were analyzed as methyl ester derivatives by gas-chromatography mass spectrometry, as described (17). Separation was performed in a SP2330 capillary column (30 m × 0.25 mm × 0.20 μm) in a GC Hewlett Packard 6890 Series II gas chromatograph (Agilent). A Hewlett Packard 5973A MS was used as the detector in the electron-impact mode. Identification of fatty acyl methyl esters was made by comparison with authentic standards and on the basis of mass spectra. Results are expressed as mol percent.

## Statistical Analysis

All statistical analyses were performed using the SPSS software (SPSS, Inc, Chicago, IL). Once normality of distribution was assessed by the Kolmogorov-Smirnov test, differences between groups (AGD samples versus controls) were analyzed with Student *t* tests, and correlations between variables were evaluated by the Pearson statistic. For comparison between AGD, AD-only, and controls, analysis of variance was performed with Tukey post hoc analyses to determine differences between groups.

## RESULTS

### Unfolded Protein Response and ER Stress in AGD

Protein misfolding associated with neurodegenerative diseases often induces ER stress (8, 9). Therefore, we examined ER stress in AGD, including the ER stress transducers PKR-like ER protein kinase (PERK), evaluated through phosphorylated eukaryotic translation initiation factor 2 α subunit (p-eIF-2α), inositol requiring 1 protein (IRE1), and activating transcription factor 6 (ATF6).

The ratio p-eIF-2α/eIF-2α was increased 5.7-fold ($p < 0.007$) in AGD cases versus controls (Fig. 1A). Increased intensity for the 3 ER stress signaling molecules IRE1, ATF6, and X-box binding protein 1 (XBP1) was detected in the AGD-affected hippocampus, where density exceeded 3.4-fold for IRE1 ($p < 0.0002$), 2.5-fold for the entire ATF6 form ($p < 0.002$), 3.2-fold for the cleaved ATF6 form ($p < 0.001$), and 3.7-fold for the IRE1 activated XBP1 ($p < 0.001$) versus controls (Fig. 1A).

Because chaperones are required during unfolded protein response (UPR) resolution (10, 11), immunoblot analyses were performed to examine several ER chaperones and folding enzymes. We found a 2- to 6-fold increase in the expression of chaperones Grp78/BiP ($p < 0.001$), Grp94 ($p < 0.002$),

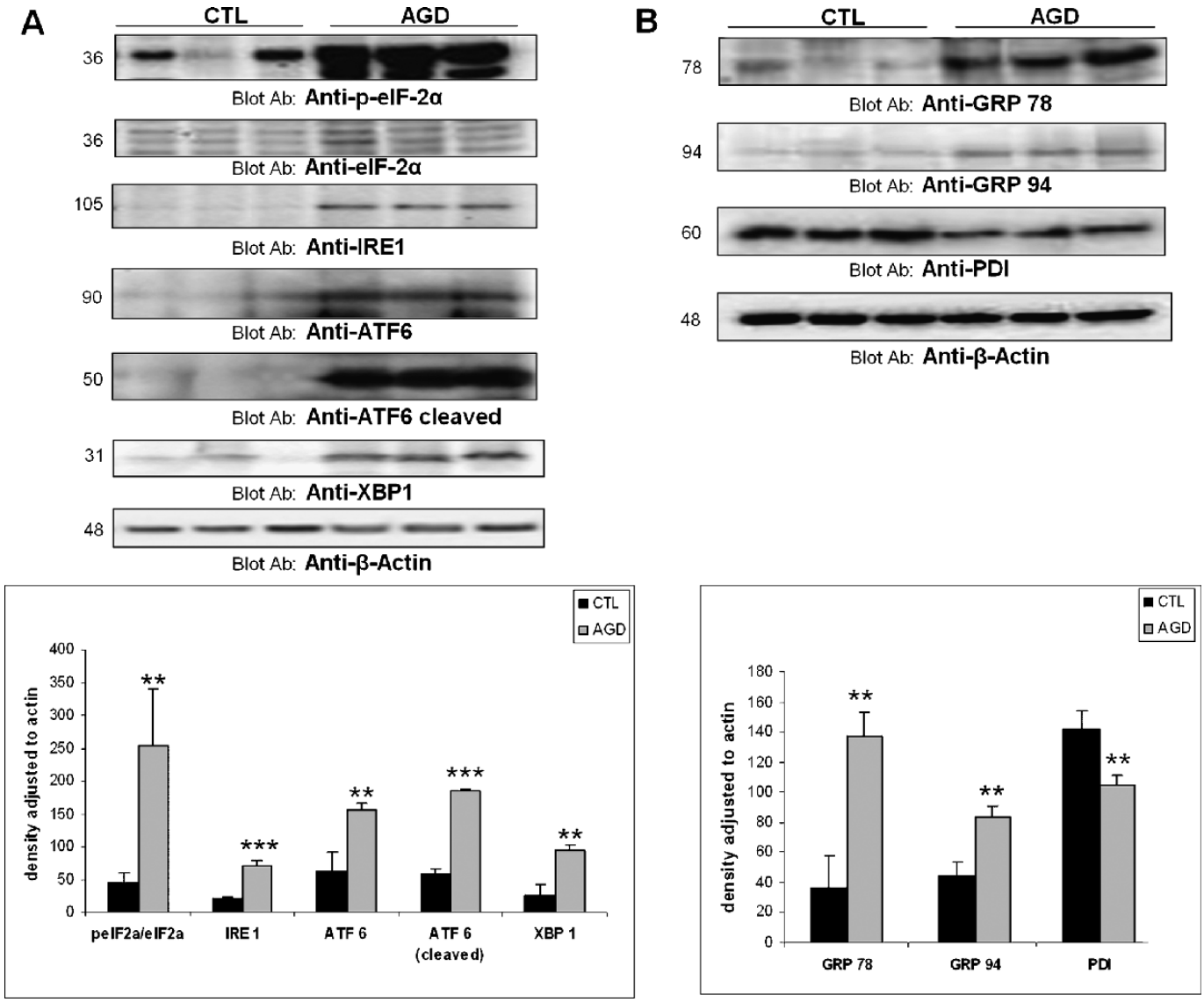


**FIGURE 1.** Endoplasmic reticulum (ER) stress in hippocampus of argyrophilic grain disease (AGD) cases. **(A, B)** Representative immunoblots of hippocampus homogenates showing increased eukaryotic translation initiation factor 2 a subunit (eIF-2α) (Ser 51) phosphorylation, inositol requiring 1 protein (IRE1) expression, activating transcription factor 6 (ATF6) cleavage and X-box binding protein 1 (XBP1) stabilization **(A)**, increased expression of ER-resident chaperones Grp78/BiP and Grp94, and decreased protein disulfide isomerase (PDI) expression **(B)**. The lower panels show quantification of the blots by densitometry normalized to actin content and significant differences between AGD cases and controls (CTL): *, $p < 0.05$; **, $p < 0.001$; and ***, $p < 0.0001$ by Student *t* test.

and KDEL-containing proteins (data not shown) in hippocampus of AGD patients (Fig. 1B). This was accompanied by a marked reduction of the foldase protein disulfide isomerase (PDI) in AGD cases ($p < 0.004$; Fig. 1B).

## Protein Oxidative Modifications in Human Hippocampus of AGD

Protein carbonyl content was increased 1.5-fold in AGD-affected hippocampus with respect to the control group ($p < 0.02$; Fig. 2A), but differences in the levels of CEL and CML were not seen between the groups (Fig. 2A); however, analysis of some bands showed increased values (Figure, Supplemental Digital Content 1, http://links.lww.com/NEN/A206).

A highly selective mass spectrometry-based technique was also used to analyze protein oxidative modifications. No significant differences in CEL and CML concentrations or in products derived from direct protein oxidation (AASA and GSA) between AGD cases and corresponding controls were identified (Fig. 2B). Only the MDAL concentration was significantly increased in the AGD hippocampus when compared with controls ($p < 0.01$; Fig. 2B).

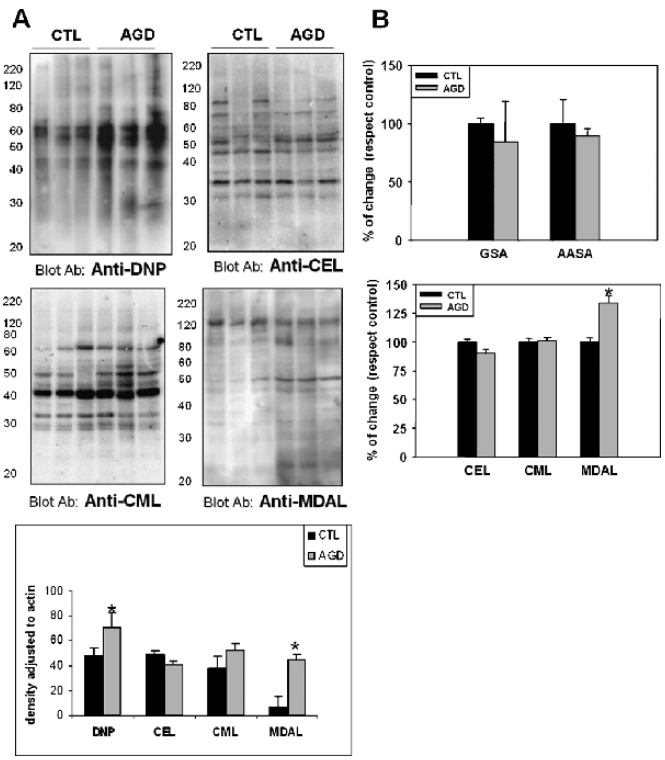


**FIGURE 2.** Protein modifications resulting from oxidative damage in argyrophilic grain disease (AGD). **(A)** Representative immunoblots for protein reactive carbonyls (anti-DNP), glycoxidation (anti–*N*ε-carboxyethyl-lysine (CEL), mixed glycoxidation/lipoxidation (anti–*N*ε-carboxymethyl-lysine [CML]), and lipoxidation (anti–*N*ε-malondialdehyde-lysine [MDAL]) reveal differential targets for each of these oxidative pathways. Apparent molecular weights are indicated. **(B)** Proteins from AGD samples show a significant increase in the amounts of lipoxidation marker MDAL, but not in the direct oxidation markers glutamic semialdehyde (GSA) and aminoadipic semialdehyde (AASA) or in glycoxidation/lipoxidation markers CEL and CML, measured by mass spectrometry. Values shown are percent changes of mean ± SEM over values in controls (CTL) (GSA: 22175 ± 1104 μmol/mol lys; AASA: 87 ± 18 μmol/mol lys; CEL: 279 ± 7 μmol/mol lys; CML: 1026 ± 35 μmol/mol lys; MDAL: 248 ± 9 μmol/mol lys). The lower panel shows densitometry quantification after band densities were normalized to actin content. *, $p < 0.05$ and **, $p < 0.001$ by Student *t* test.

## Characterization of Advanced Glycation Endproducts-Modified Proteins

Advanced glycation endproducts immunostaining and CML immunoblot analyses demonstrated some specific alterations in AGD. The CML-modified proteins were identified after 2-dimensional electrophoresis with matrix-assisted laser desorption/ionization time-of-flight mass spectrometry; 2 modified isoforms of fructose-bisphosphate aldolase A and C were increased in AGD, and 1 phosphatidyl-ethanolamine-binding protein was decreased in AGD compared with controls (Fig. 3).

## Fatty Acid Composition and Lipoxidative Modification of Proteins in AGD

The high content of polyunsaturated fatty acids in the central nervous system along with its elevated oxygen consumption supports the possible significance of lipid peroxidation–derived processes in neurodegeneration. Only nonsignificant differences versus controls in hippocampal fatty acid levels were noted in AGD cases (Table 3), but the lipoxidation marker MDAL was 1.5-fold higher in AGD patients versus controls ($p < 0.001$; Fig. 2A).

## Mitochondrial Dysfunction and Antioxidant Defense in AGD

Because mitochondria are a major free radical source (24), expression levels of representative subunits of mitochondrial respiratory complexes I to IV (25, 26) were analyzed by gel electrophoresis and Western blotting.

Complex I (NUDFS3 subunit) and IV (MTCO1 subunit) were significantly decreased 1.4-fold ($p < 0.04$) and 1.9-fold ($p < 0.02$), respectively, in AGD versus controls. Yet, no significant changes were observed for subunits of respiratory complexes II (SDHA subunit) and III (UQCRC2 subunit) (Fig. 4).

Uncoupling protein 4 (UCP4), a mitochondrial protein specific for brain tissue that modulates neuronal energy metabolism by increasing glucose uptake and shifting the mode of ATP production from mitochondrial respiration to glycolysis (26), can contribute to decreased free radical leak. Levels of UCP4 were found to be significantly decreased in AGD compared with controls ($p < 0.01$; Fig. 4). The apoptosis-inducing factor (another multifunctional mitochondrial protein involved in oxidative stress as an reactive oxygen species scavenger, maintenance of mitochondrial complex structure [27], and cell death) showed a 3.7-fold increase in AGD-affected samples versus controls ($p < 0.001$; Fig. 4). Porin levels normalized to actin content decreased 1.2-fold ($p < 0.04$) in AGD cases versus controls (Fig. 4).

Double-labeling immunofluorescence of porin or COX subunit IV and phospho-tau (tau-P) showed no colocalization of mitochondrial markers in grains (Fig. 5).

To delineate a potential response targeting mitochondria further, the nuclear respiratory factor 1 (Nrf1; encoding

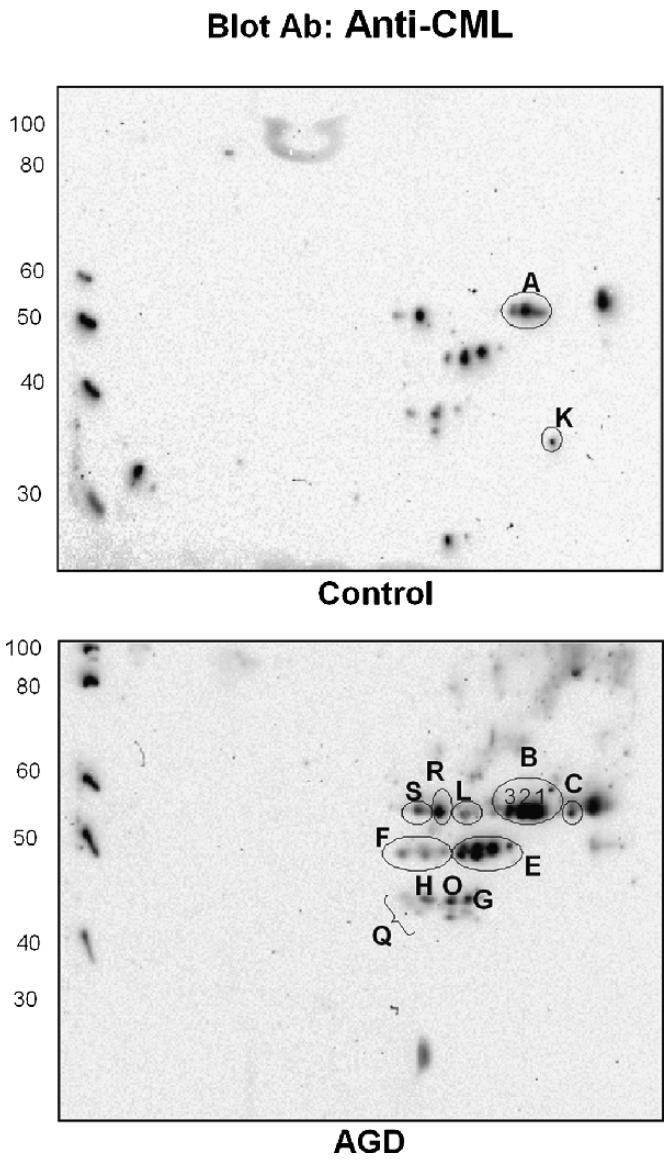


**FIGURE 3.** Identification of argyrophilic grain disease (AGD)–modified proteins 2-dimensional gel electrophoresis and immunoblotting of membranes stained with anti–*N*ε-carboxymethyl-lysine (CML). Densitometric analyses, after normalization to protein content quantified by silver stain, demonstrated differentially stained spots (marked by letters a to s). Numbers indicate apparent molecular weights. Two-dimensional gels processed in parallel and stained with silver were also used to obtain the spots for mass spectrometry analysis. Dissection of the spots and their analyses revealed several isoforms of fructose bisphosphate aldolase (access number P04075; P09972) and phosphatidylethanolamine-binding protein (access number P30086).

nuclear genes required for respiration, heme biosynthesis, and mitochondrial DNA transcription and replication) was analyzed. Nuclear factor (erythroid-derived 2)-like 2 (NRF2), activating the stress-dependent expression genes such as *SOD1* and *SOD2* through an antioxidant responsive element (28), was also evaluated. Nrf1 and NRF2 were increased in AGD versus controls 2.2-fold ($p < 0.01$) and 8.5-fold ($p < 0.007$), respectively (Fig. 6). Immunohistologic staining of antioxidants SOD1 and SOD2, NRF2-regulated genes, demonstrated a marked increase in hippocampus of AGD patients (Fig. 6).

To investigate whether mitochondrial biogenesis was affected in AGD, levels of mitochondrial transcriptional factor A (TFAM) and mitochondrial fusion protein-1 were used as mitochondrial biogenesis markers. No differences in the expression levels of these proteins were found between the AGD and control groups (Fig. 6A). Finally, to shed further light on a potential dysregulation of mitochondria, levels of sirtuin 1 (SIRT1), activator of peroxisome proliferator–activated receptor γ coactivator 1 (PGC1α), and receptor interacting protein 140 (RIP140) (negative regulator of mitochondrial biogenesis) were analyzed. The levels of SIRT1 were decreased 2.4-fold ($p < 0.01$) (Fig. 6B), whereas the

**TABLE 3.** Fatty Acid Profile and Derived Indices in Hippocampal Cortex Samples

| | Control Group | AGD Group | p |
|---|---|---|---|
| 14:0 | 0.41 ± 0.10 | 0.58 ± 0.02 | 0.085 |
| 16:0 | 19.56 ± 0.1 | 18.83 ± 0.23 | 0.056 |
| 16:1n-7 | 0.94 ± 0.15 | 0.70 ± 0.04 | 0.114 |
| 18:0 | 21.87 ± 0.0 | 22.08 ± 0.26 | 0.553 |
| 18:1n-9 | 26.62 ± 0.1 | 27.11 ± 0.25 | 0.180 |
| 18:2n-6 | 0.60 ± 0.01 | 0.48 ± 0.10 | 0.058 |
| 18:3n-3 | 0.18 ± 0.01 | 0.20 ± 0.01 | 0.300 |
| 20:0 | 1.51 ± 0.05 | 2.16 ± 0.23 | 0.060 |
| 20:1 | 0.35 ± 0.00 | 0.32 ± 0.02 | 0.239 |
| 20:2n-6 | 0.19 ± 0.08 | 0.30 ± 0.08 | 0.080 |
| 20:3n-6 | 0.95 ± 0.18 | 0.73 ± 0.05 | 0.205 |
| 20:4n-6 | 7.55 ± 0.10 | 7.46 ± 0.26 | 0.806 |
| 22:4n-6 | 6.31 ± 0.14 | 5.52 ± 0.20 | 0.054 |
| 22:5n-6 | 0.79 ± 0.06 | 0.73 ± 0.05 | 0.471 |
| 22:5n-3 | 0.35 ± 0.09 | 0.57 ± 0.07 | 0.068 |
| 22:6n-3 | 11.06 ± 0.2 | 11.36 ± 0.18 | 0.346 |
| 24:0 | 0.39 ± 0.05 | 0.47 ± 0.005 | 0.117 |
| 24:1n-9 | 0.29 ± 0.07 | 0.31 ± 0.008 | 0.690 |
| ACL | 18.56 ± 0.00 | 18.58 ± 0.01 | 0.378 |
| SFA | 43.75 ± 0.15 | 44.13 ± 0.24 | 0.286 |
| UFA | 56.24 ± 0.15 | 55.86 ± 0.24 | 0.286 |
| MUFA | 28.22 ± 0.09 | 28.46 ± 0.21 | 0.423 |
| PUFA | 28.01 ±0.06 | 27.40 ± 0.28 | 0.126 |
| PUFAn = 6 | 16.41 ± 0.29 | 15.25 ± 0.43 | 0.085 |
| PUFAn = 3 | 11.60 ± 0.24 | 12.14 ± 0.17 | 0.100 |
| DBI | 160.8 ± 4 0.3 | 159.58 ± 0.81 | 0.272 |
| PI | 157.67 ± 1.0 | 154.14 ± 0.94 | 0.721 |

Values shown are mean ± SEM.

Fatty acid indexes were calculated as follows: saturated fatty acids (SFA), unsaturated fatty acids (UFA), monounsaturated fatty acids (MUFA), polyunsaturated fatty acids from n-3 and n-6 series (PUFAn-3 and PUFAn-6), average chain length (ACL) = [(∑%Total 14 × 14) + (∑%Total 16 × 16) + (∑%Total 18 × 18) + (∑%Total 20 × 20) + (∑%Total 22 × 22)] / 100]; double-bond index (DBI) = [(1 × ∑mol% monoenoic) + (2 × ∑mol% dienoic) + (3 × ∑mol% trienoic) + (4 × ∑mol% tetraenoic) + (5 × ∑mol% pentaenoic) + (6 × ∑mol% hexaenoic)], and peroxidizability index (PI) = [(0.025 × ∑mol% monoenoic) + (1 × ∑mol% dienoic) + (2 × ∑mol% trienoic) + (4 × ∑mol% tetraenoic) + (6 × ∑mol% pentaenoic) + (8 × ∑mol% hexaenoic)].

AGD, argyrophilic grain diseases.

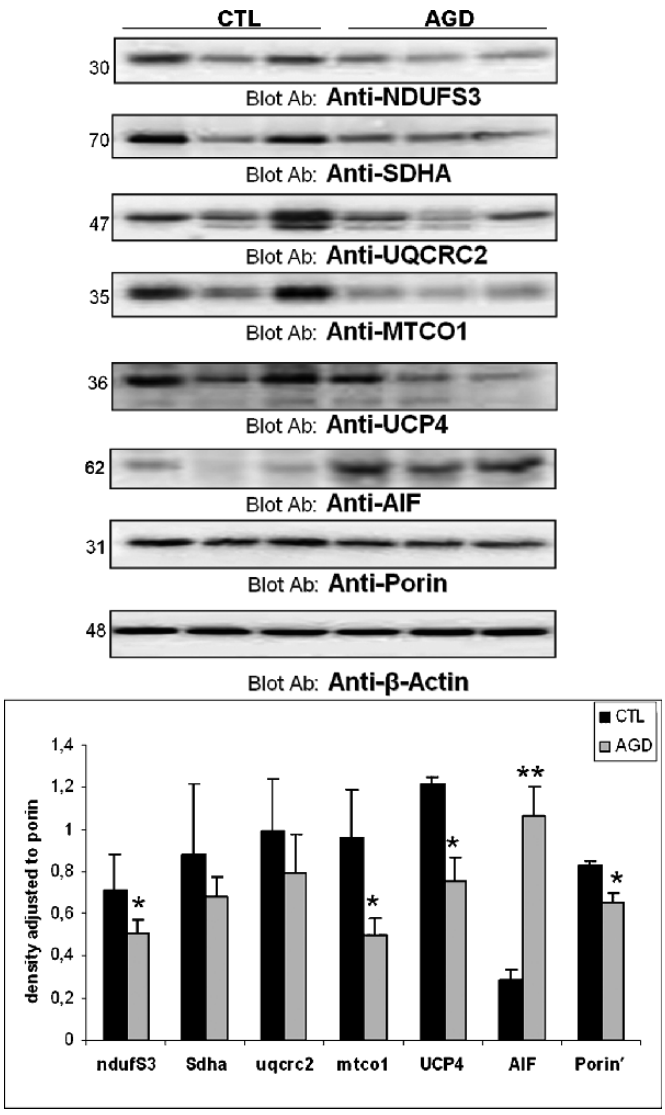


**FIGURE 4.** Expression levels of mitochondria-related proteins. Representative immunoblots of peptides NDUFS3, SDHA, core 2 UQCRC2, and MTCO1, subunits of mitochondrial respiratory chain complexes I, II, III, and IV, respectively, suggesting decreased complex I and IV contents in hippocampus of argyrophilic grain disease (AGD) cases versus controls (CTL). This was associated with increased expression of apoptosis-inducing factor (AIF) and decreased contents of uncoupling protein 4 (UCP4) and porin. The lower panel shows the quantification of blots by densitometry after band densities were normalized to porin content. Differences versus control group were determined by Student *t* test (*, $p < 0.05$ and **, $p < 0.001$).

levels of both PGC1α and RIP140 were increased 3-fold ($p < 0.0001$) and 2.7-fold ($p < 0.002$), respectively, in AGD cases versus controls (Figs. 6A, B).

### Selectivity of AGD Changes Versus AD

Because AGD is often associated with AD and the AGD cases in this series also had some AD pathology, we examined several AD-only samples (i.e. without grains) to ascertain whether the changes identified were attributable to the presence of AD. These analyses demonstrated that oxidative stress and ER stress were also present in the examined AD patients (data not shown). However, the degree of PDI loss was not as marked in AD samples as in AGD (Fig. 7B). Furthermore, increased expression of PGC1α was significantly lower in AD-only than in AGD samples (Fig. 7B). Most strikingly, although AGD samples showed decreased contents of mitochondrial complexes I, II, and IV, in AD-only samples, a significant increment of levels of complex I, II, and IV representative peptides was evident (Fig. 7A).

## DISCUSSION

The present study was designed to gain understanding of AGD pathogenesis. Because AGD is often associated with AD lesions, we compared AGD and nonpathologic control samples and performed an AGD/AD-AD comparison in which AGD cases were restricted to those with limited AD-related pathology and in which the AD-only cases had similar stages of AD-related pathology without grains. Although limited in numbers of cases, the present series may be adequate to explore AGD-specific changes.

Previous studies have shown accumulation of hyperphosphorylated tau and truncated tau, altered ubiquitin-proteasome system with p62/sequestosome 1, and ubiquitin colocalization with abnormal tau and with accompanying expression of mutant ubiquitin in AGD (1). Furthermore, tau hyperphosphorylation is associated with the activation of stress kinases p38 and SAPK/JNK (29), thus indicating possible triggering by oxidative stress. On the basis of those observations, we analyzed aspects related to abnormal protein aggregation and ER stress, oxidative stress, and mitochondrial alteration and biogenesis in AGD.

The ER is a central organelle involved in several molecular pathways including lipid synthesis and protein synthesis, folding, and maturation. Conditions interfering with ER function result in ER stress, which may be caused by excessive protein production or by the accumulation of unfolded protein aggregates, giving rise to the UPR. Activation of the ER transmembrane proteins IRE1, ATF6, and PERK characterizes the UPR (30, 31). Signaling through ATF6 induces XBP1 transcription, which provides positive feedback for UPR activation (30). We found increased expression levels of 3 stress signaling molecules, namely, IRE1, ATF6, and XBP1, in the hippocampus in AGD cases compared with that in controls. The last key protein, PERK, is considered the major eIF-2α phosphorylation regulator during the UPR, phosphorylating and inactivating eIF-2α, and blocking the translational initiation of the proteins to prevent their accumulation in the ER lumen (32–35). In line with other data, the p-eIF-2α/eIF-2α ratio was increased in AGD, thus indirectly suggesting increased PERK activity.

Endoplasmic reticulum stress mediates the expression of foldases and $Ca^{2+}$-dependent molecular chaperones such as PDI, Grp78/BiP, and Grp94 that protect cells from ER stress damage (36, 37). Grp78/BiP and Grp94 expression levels were increased in the hippocampus in AGD patients; however, this was accompanied by a marked reduction of the foldase protein PDI.

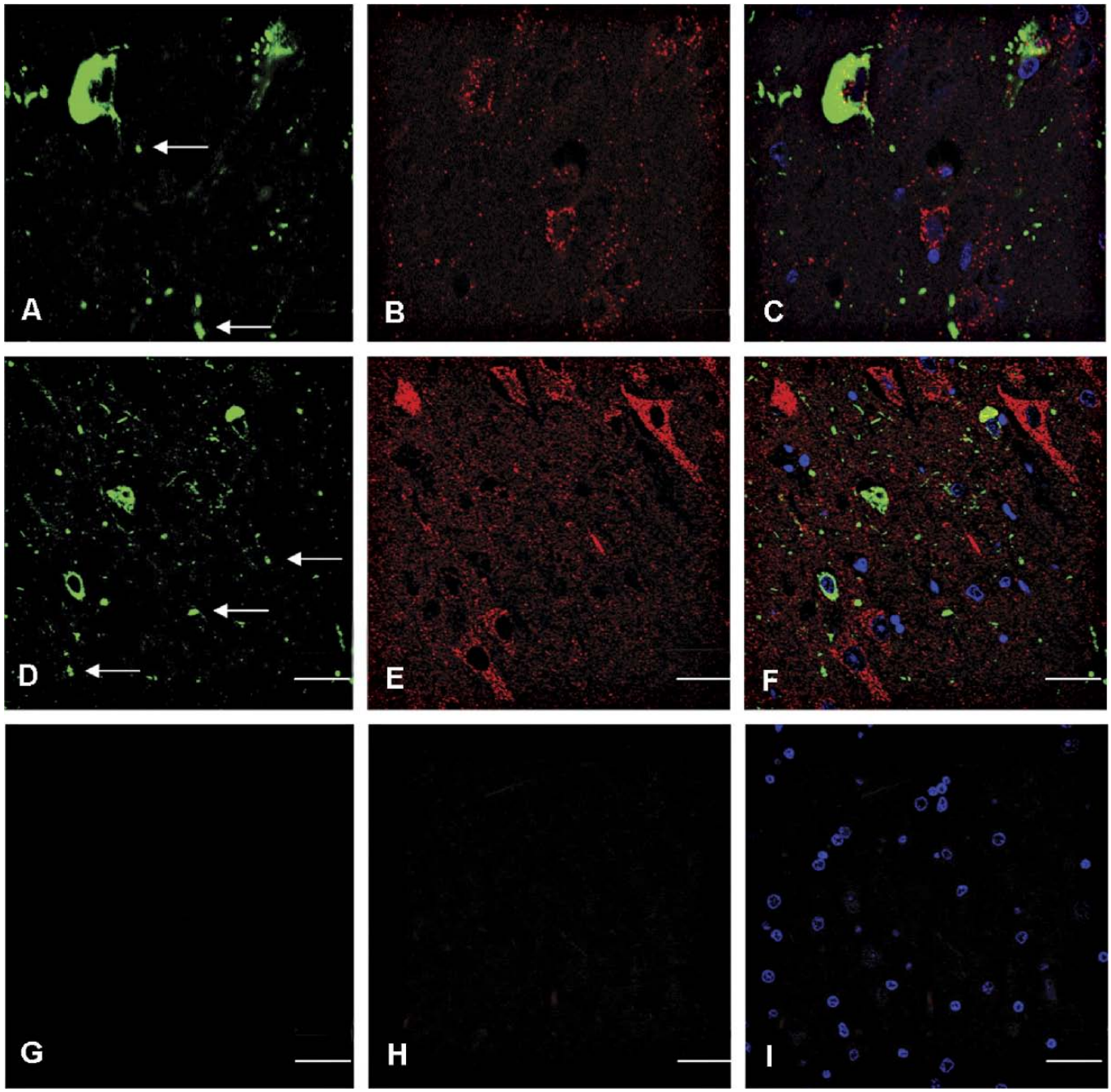


**FIGURE 5.** Lack of colocalization of tau with porin in grains. **(A–C)** tau-P (**A**, green) and mitochondrial porin (**B**, red) showing no colocalization in grains (**C**, merge). **(D–F)** tau-P (**D**, green) and cytochrome *C* oxidase subunit IV (**E**, red) showing no colocalization of Cox with tau-P in grains. **(G–I)** Parallel sections immunostained without the primary antibodies are used as negative controls. Nuclei are stained with TO-PRO.

Among the markers of oxidative stress evaluated, the concentration of the lipoxidation marker MDAL was significantly increased, together with that of protein reactive carbonyls (DNP). However, markers of direct protein oxidation (AASA and GSA) and markers of glycoxidation (CEL and CML) were not altered in AGD when compared with the non-AGD cases bearing similar AD-related changes. Increased MDAL levels suggest relevant lipid peroxidation in AGD. This is further supported by the slight modification of the lipid profile in AGD cases compared with that of controls, although no significant differences were seen in levels of monounsaturated and polyunsaturated fatty acids, double-bond index, and peroxidizability index in AGD compared with controls (Table 3).

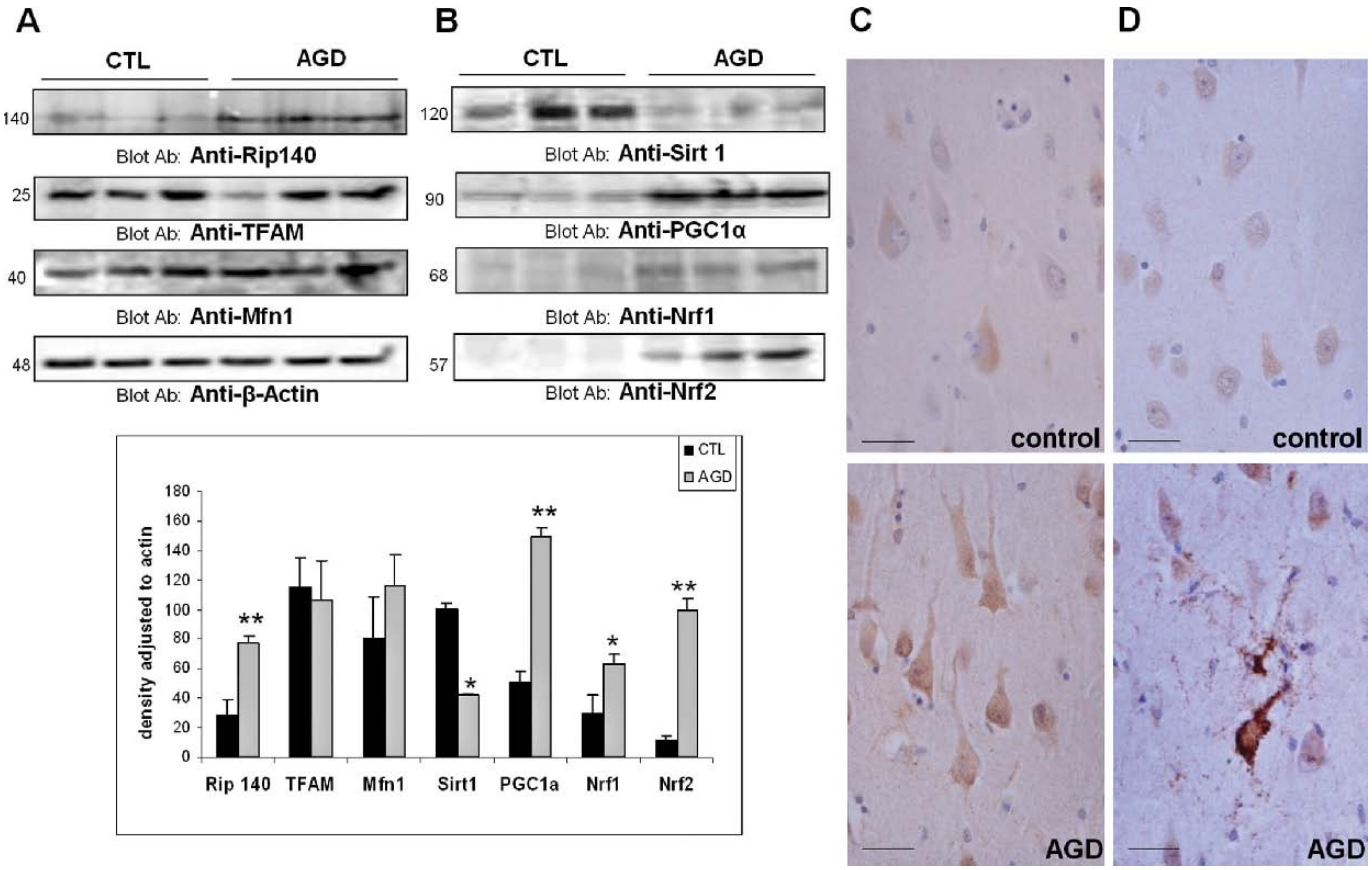


**FIGURE 6.** Antioxidant response and mitochondrial biogenesis dysfunction in hippocampus of argyrophilic grain disease (AGD) cases. **(A, B)** Lack of effective biogenetic response is indicated by representative immunoblots revealing unchanged levels of mitochondrial biogenesis mediators mitochondrial transcriptional factor A (TFAM) and mitochondrial fusion protein-1 (Mfn1), and increased amount versus control (CTL) of mitochondrial biogenesis corepressor receptor interacting protein 140 (RIP140) **(A)**. This may be reinforced by lowered levels of the peroxisome proliferator–activated receptor γ coactivator 1 (PGC1α) regulator sirtuin 1 (SIRT1) despite the increased levels of positive mitochondrial biogenesis coactivator PGC1α and nuclear respiratory factor 1 (Nrf1) **(B)**. The downstream antioxidant response component NRF2 was also increased. The lower panel shows quantification of blots by densitometry after band densities were normalized to actin content. Differences were analyzed versus the CTL group by Student *t* test (*, $p < 0.05$ and **, $p < 0.001$). Immunohistochemical images of antioxidant response components (related to NRF2) such as superoxide dismutase 1 (SOD1) **(C)** and SOD2 **(D)** in CA1 area of the hippocampus showing increased expression in AGD versus controls. Bar = 25 μm.

Targets of oxidative damage were fructose-bisphosphate aldolase, which catalyzes the enzymatic cleavage of β-d-fructose-1,6-bisphosphate leading to the formation of glyceraldehyde 3-phosphate, the major source of methylglyoxal (38). The other identified protein, phosphatidyl-ethanolamine-binding protein, is an individual signaling protein (39) that may act as an inhibitor of the chymotrypsin-like activity of the proteasome (40). The specificity of these modifications must be approached with caution because hundreds of proteins are targets of oxidation in human neurodegenerative diseases (41, 42).

Because mitochondria are a major source of free radicals (24), expression levels of representative subunits of mitochondrial respiratory complexes I to IV (25, 26) were analyzed by gel electrophoresis and Western blotting. Expression levels of complex I and IV subunits were decreased in AGD cases. Moreover, UCP4 (a mitochondrial protein specific for brain tissue that modulates neuronal energy metabolism by increasing glucose uptake and shifting the mode of ATP production from mitochondrial respiration to glycolysis [26]) was also reduced in AGD. Expression of apoptosis inducing factor, another multifunctional mitochondrial protein involved in oxidative stress and mitochondrial structure (27), is increased in AGD. Together, these observations point to impaired mitochondrial function in AGD. There was also increased expression of NRF2, activating the stress-dependent expression genes *SOD1* and *SOD2* through an antioxidant responsive element (28). Nrf1, NRF2, SOD1, and SOD2 levels were elevated in AGD hippocampi compared with controls.

In addition to oxidative stress, ER stress can also trigger NRF2 (31). Moreover, PGC1α is also an upstream signal for NRF2 activation and a major regulator of the antioxidant defense. The present findings show that it is elevated in AGD, thus contributing to the development of antioxidative and anti–ER stress responses.

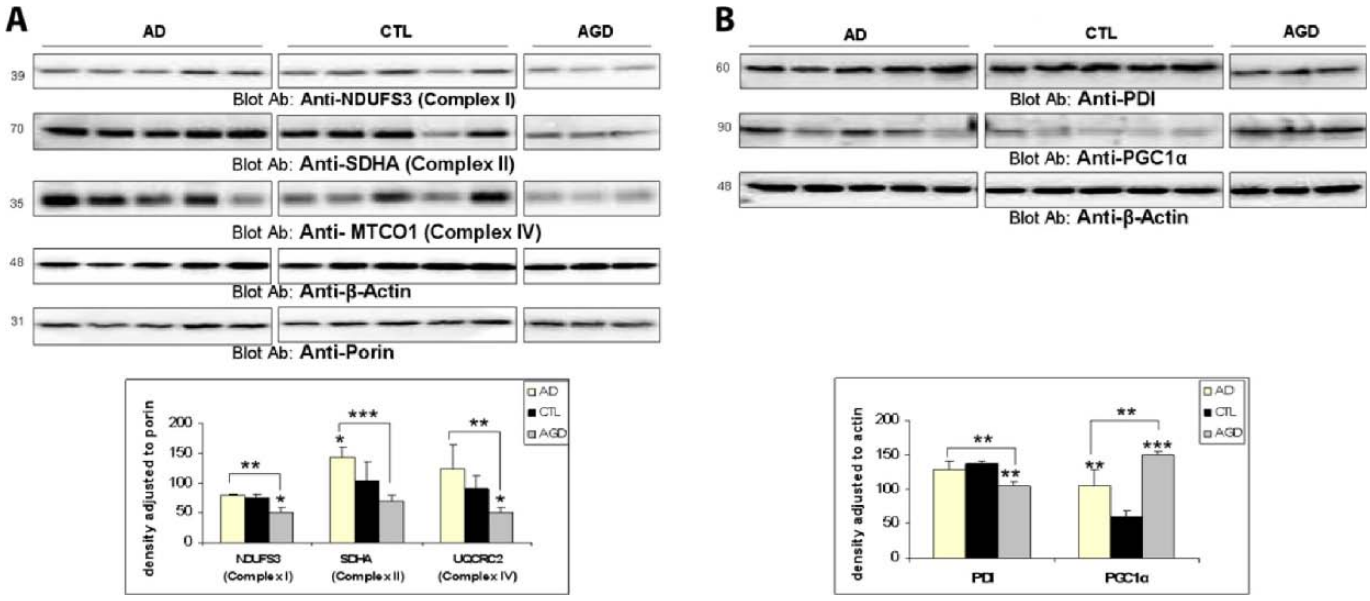


**FIGURE 7.** Specificity of argyrophilic grain disease (AGD) changes in comparison to Alzheimer disease (AD). **(A)** Representative immunoblots of mitochondrial respiratory chain complexes subunits NDUFS3 (complex I), SDHA (complex II), and MTCO1 (complex IV) in AD and AGD samples, suggesting decreased complex I and IV contents in hippocampus of AGD and increased complex II content in hippocampus of AD cases versus controls. Direct comparison of Western blot analyses of mitochondrial peptides from AD and AGD samples shows statistically significant differences between both AD and AGD cases. The lower panel shows the quantification by densitometry after band densities were normalized to porin content. **(B)** Representative immunoblots of endoplasmic reticulum (ER) marker protein disulfide isomerase (PDI) and mitochondrial biogenesis coactivator peroxisome proliferator–activated receptor γ coactivator 1 (PGC1α) in AD and AGD samples show decreased PDI levels in AGD, whereas PDI levels are unchanged in AD and increased PGC1α in AD and AGD cases, although there is statistically significant differences between both groups. The lower panel shows quantification by densitometry after band densities were normalized to actin content. Differences were analyzed with respect to control or AD-only group by analysis of variance and Tukey post hoc analyses (*, $p < 0.05$; **, $p < 0.001$; and ***, $p < 0.0001$).

We speculated that mitochondrial biogenesis could be increased as a compensatory mechanism of impaired mitochondrial function of certain respiratory chain complexes. PGC1α is also a regulator of mitochondrial biogenesis (43, 44). However, levels of mitochondrial transcriptional factor (TFAM) and mitochondrial fusion protein-1 (mitochondrial biogenesis activators) were reduced, whereas RIP140, a negative regulator of mitochondrial biogenesis (45), was increased. Therefore, our observations indicate impaired mitochondrial biogenesis in AGD, a feature supported by reduced levels of mitochondrial porin. Interestingly, no porin was expressed in grains, as revealed by double-labeling immunofluorescence and confocal microscopy, which contrasts with the accumulation of mitochondrial porin and altered mitochondria in dystrophic neurites of senile plaques in AD (46). Another puzzling aspect was the observation that the major activity regulator of PGC1α, SIRT1 (47, 48), was depleted; this is a surprising finding in the context of increased PGC1α in AGD. Whether SIRT1 multimodal functions of sirtuins in neurodegeneration (49) may explain this unexpected finding in AGD is an open question.

In summary, we have shown in that, in AGD, there is 1) ER stress, activation of UPR, and activation of ER stress responses; 2) oxidative stress damage mainly related to lipoxidative (MDAL-related) lesions and increased oxidative stress responses; 3) selective alteration of subunits of complex I and IV of the respiratory chain and altered expression of proteins that regulate neuronal energy metabolism by increasing glucose uptake and shifting the mode of ATP production (together with activation of molecular pathways that lead to the production of oxidative stress responses); and 4) alteration of mitochondrial biogenesis resulting from reduced expression of inductors of mitochondrial biogenesis and upregulation of repressors. Furthermore, although limited by sample size, we show that some changes (i.e. of PDI, PGC1α and selective alteration of subunits of mitochondrial complexes) may be exclusive to AGD, thereby reinforcing the concept of molecular specificity of this disease in comparison with other tauopathies.

## ACKNOWLEDGMENTS

*The authors thank the tissue donors and their families and Dr Jesus Requena (Universidad de Santiago de Compostela, Spain) for providing the GSA and AASA standards.*

## REFERENCES

1. Ferrer I, Santpere G, van Leeuwen FW. Argyrophilic grain disease. Brain 2008;131:1416–32
2. Tolnay M, Clavaguera F. Argyrophilic grain disease: A late-onset dementia with distinctive features among tauopathies. Neuropathology 2004;24:269–83

3. Tolnay M, Probst A. Argyrophilic grain disease. Handb Clin Neurol 2008;89:553–63
4. Serrano F, Klann E. Reactive oxygen species and synaptic plasticity in the aging hippocampus. Ageing Res Rev 2004;3:431–43
5. Gray DA, Tsirigotis M, Woulfe J. Ubiquitin, proteasomes, and the aging brain. Sci Aging Knowledge Environ 2003;2003:RE6
6. Trojanowski JQ, Mattson MP. Overview of protein aggregation in single, double, and triple neurodegenerative brain amyloidoses. Neuromolecular Med 2003;4:1–6
7. Scarpulla RC. Transcriptional paradigms in mammalian mitochondrial biogenesis and function. Physiol Rev 2008;88:611–38
8. Sitte N, Huber M, Grune T, et al. Proteasome inhibition by lipofuscin/ceroid during postmitotic aging of fibroblasts. FASEB J 2000;14:1490–98
9. Grune T, Jung T, Merker K, et al. Decreased proteolysis caused by protein aggregates, inclusion bodies, plaques, lipofuscin, ceroid, and 'aggresomes' during oxidative stress, aging, and disease. Int J Biochem Cell Biol 2004;36:2519–30
10. Dean RT, Fu S, Stocker R, et al. Biochemistry and pathology of radical-mediated protein oxidation. Biochem J 1997;324:1–18
11. Stadtman ER, Berlett BS. Reactive oxygen–mediated protein oxidation in aging and disease. Drug Metab Rev 1998;30:225–43
12. Hawkins CL, Davies MJ. Generation and propagation of radical reactions on proteins. Biochim Biophys Acta 2001;1504:196–219
13. Requena JR, Fu MX, Ahmed MU, et al. Quantification of malondialdehyde and 4- hydroxynonenal adducts to lysine residues in native and oxidized human low-density lipoprotein. Biochem J 1997;322:317–25
14. Baynes JW. Chemical modification of proteins by lipids in diabetes. Clin Chem Lab Med 2003;41:1159–65
15. Marciniak SJ, Ron D. Endoplasmic reticulum stress signaling in disease. Physiol Rev 2006;86:1133–49
16. Zhang K, Kaufman RJ. The unfolded protein response: A stress signaling pathway critical for health and disease. Neurology 2006;66:S102–9
17. Pamplona R, Dalfo E, Ayala V, et al. Proteins in human brain cortex are modified by oxidation, glycoxidation, and lipoxidation. Effects of Alzheimer disease and identification of lipoxidation targets. J Biol Chem 2005;280:21522–30
18. Dalfo E, Portero-Otin M, Ayala V, et al. Evidence of oxidative stress in the neocortex in incidental Lewy body disease. J Neuropathol Exp Neurol 2005;64:816–30
19. Muntane G, Dalfo E, Martinez A, et al. Glial fibrillary acidic protein is a major target of glycoxidative and lipoxidative damage in Pick's disease. J Neurochem 2006;99:177–85
20. Ilieva EV, Ayala V, Jove M, et al. Oxidative and endoplasmic reticulum stress interplay in sporadic amyotrophic lateral sclerosis. Brain 2007;130:3111–23
21. Ferrer I, Barrachina M, Tolnay M, et al. Phosphorylated protein kinases associated with neuronal and glial tau deposits in argyrophilic grain disease. Brain Pathol 2003;13:62–78
22. van der Vlies D, Woudenberg J, Post JA. Protein oxidation in aging: Endoplasmic reticulum as a target. Amino Acids 2003;25:397–407
23. Ferrer I, Martinez A, Boluda S, et al. Brain banks: Benefits, limitations and cautions concerning the use of post-mortem brain tissue for molecular studies. Cell Tissue Bank 2008;9:181–94
24. Pamplona R, Barja G. Highly resistant macromolecular components and low rate of generation of endogenous damage: Two key traits of longevity. Ageing Res Rev 2007;6:189–210
25. Chen Q, Vazquez EJ, Moghaddas S, et al. Production of reactive oxygen species by mitochondria: Central role of complex III. J Biol Chem 2003;278:36027–31
26. Liu D, Chan SL, de Souza-Pinto NC, et al. Mitochondrial UCP4 mediates an adaptive shift in energy metabolism and increases the resistance of neurons to metabolic and oxidative stress. Neuromolecular Med 2006;8:389–414
27. Klein JA, Ackerman SL. Oxidative stress, cell cycle, and neurodegeneration. J Clin Invest 2003;111:785–93
28. Cullinan SB, Diehl JA. Coordination of ER and oxidative stress signaling: The PERK/Nrf2 signaling pathway. Int J Biochem Cell Biol 2006;38:317–32
29. Ferrer I, Barrachina M, Tolnay M, et al. Phosphorylated protein kinases associated with neuronal and glial tau deposits in argyrophilic grain disease. Brain Pathol 2003;13:62–78
30. Xu C, Bailly-Maitre B, Reed JC. Endoplasmic reticulum stress: Cell life and death decisions. J Clin Invest 2005;115:2656–64
31. Kaufman RJ. Orchestrating the unfolded protein response in health and disease. J Clin Invest 2002;110:1389–98
32. Proud CG. eIF2 and the control of cell physiology. Semin Cell Dev Biol 2005;16:3–12
33. Wek RC, Jiang HY, Anthony TG. Coping with stress: eIF2 kinases and translational control. Biochem Soc Trans 2006;34:7–11
34. Wek RC, Cavener DR. Translational control and the unfolded protein response. Antioxid Redox Signal 2007;9:2357–71
35. Raven JF, Koromilas AE. PERK and PKR: Old kinases learn new tricks. Cell Cycle 2008;7:1146–50
36. Ni M, Lee AS. ER chaperones in mammalian development and human diseases. FEBS Lett 2007;581:3641–51
37. Wang M, Ye R, Barron E, et al. Essential role of the unfolded protein response regulator GRP78/BiP in protection from neuronal apoptosis. Cell Death Differ 2010;17:488–98
38. Hamada Y, Araki N, Koh N, et al. Rapid formation of advanced glycation end products by intermediate metabolites of glycolytic pathway and polyol pathway. Biochem Biophys Res Commun 1996;228:539–43
39. Weitzdorfer R, Hoger H, Shim KS, et al. Changes of hippocampal signaling protein levels during postnatal brain development in the rat. Hippocampus 2008;18:807–13
40. Chen Q, Wang S, Thompson SN, et al. Identification and characterization of PEBP as a calpain substrate. J Neurochem 2006;99:1133–41
41. Sultana R, Perluigi M, Butterfield DA. Oxidatively modified proteins in Alzheimer's disease (AD), mild cognitive impairment and animal models of AD: Role of Aβ in pathogenesis. Acta Neuropathol 2009;118:131–50
42. Martínez A, Portero-Otin M, Pamplona R, Ferrer I. Protein targets of oxidative damage in human neurodegenerative diseases with abnormal protein aggregates. Brain Pathol 2010;20:281–97
43. Cui L, Jeong H, Borovecki F, et al. Transcriptional repression of PGC-1α by mutant huntingtin leads to mitochondrial dysfunction and neurodegeneration. Cell 2006;127:59–69
44. Wu Z, Puigserver P, Andersson U, et al. Mechanisms controlling mitochondrial biogenesis and respiration through the thermogenic coactivator PGC-1. Cell 1999;98:115–24
45. White R, Morganstein D, Christian M, et al. Role of RIP140 in metabolic tissues: Connections to disease. FEBS Lett 2008;582:39–45
46. Ramírez CM, González M, Díaz M, et al. VDAC and ERα interaction in caveolae from human cortex is altered in Alzheimer's disease. Mol Cell Neurosci 2009;42:172–83
47. Nemoto S, Fergusson MM, Finkel T. SIRT1 functionally interacts with the metabolic regulator and transcriptional coactivator PGC-1α. J Biol Chem 2005;280:16456–60
48. Aquilano K, Vigilanza P, Baldelli S, et al. Peroxisome proliferator–activated receptor γ co-activator 1 α (PGC-1 α) and sirtuin 1 (SIRT1) reside in mitochondria: Possible direct function in mitochondrial biogenesis. J Biol Chem 2010;285:21590–99
49. Tang BL. Sirt1's complex roles in neuroprotection. Cell Mol Neurobiol 2009;29:1093–1103




 